A preliminary seismic catalog for the Mozambique Channel

Andry Ramarolahy
Department of Earth & Environmental Sciences, Columbia University, New York, US
aramarolahy@ldeo.columbia.edu

Andriamiranto Raveloson
Institute and Observatory of Geophysics of Antananarivo (IOGA), Antananarivo, Madagascar
rruntwo@gmail.com

Rasheed Ajala
Lamont-Doherty Earth Observatory of Columbia University, New York, US
rajala@ldeo.columbia.edu

Folarin Kolawole
Department of Earth & Environmental Sciences, Columbia University, New York, US
Lamont-Doherty Earth Observatory of Columbia University, New York, US
fola@ldeo.columbia.edu

This manuscript has been submitted for review and publication in the Journal of African Earth Sciences. It is our expectation that it will hopefully be accepted for publication. Subsequent versions of this manuscript may differ due to editorial process. If accepted for publication, the final version will be available through the "Peer-reviewed publication DOI" link on EarthArXiv. Kindly contact Andry Ramarolahy (aramarolahy@ldeo.columbia.edu) for correspondences regarding this manuscript.

A preliminary seismic catalog for the Mozambique Channel

Andry Ramarolahy[1], Andriamiranto Raveloson[2], Rasheed Ajala[3], Folarin Kolawole[1,3]

[1]Department of Earth & Environmental Sciences, Columbia University, New York, US
[3]Institute and Observatory of Geophysics of Antananarivo (IOGA), Antananarivo, Madagascar
[3]Lamont-Doherty Earth Observatory of Columbia University, New York, US

Corresponding author: aramarolahy@ldeo.columbia.edu

Keypoints:

1. We develop a preliminary earthquake catalog for the Mozambique Channel
2. Catalog shows magnitude of completeness of M_L3.5 and b-value of 0.76
3. Earthquakes collocate with known active plate boundaries and submarine volcanoes

Abstract

The Mozambique Channel is a 1,600-km long, 950 – 1,000-km wide deep-water arm of southwestern Indian Ocean, located between Mozambique and Madagascar Island. The channel hosts the offshore continuation of the East African Rift System, an active divergent plate boundary that has propagated from the African continent, across Mesozoic continental rifted margins, into Mesozoic oceanic lithosphere. The earthquake and tsunami hazards posed by the network of active plate boundaries in the Mozambique Channel necessitates a regional seismic database to aid scientific investigations, hazard analysis, and mitigation efforts. However, the Mozambique Channel lacks a systematic regional-scale analysis of event distribution, thus limiting advances in seismological investigations of the region. Here, we utilize 256 seismic stations onshore mainland Africa and in Madagascar to detect and locate earthquakes in the Mozambique Channel between 1990 and 2021, to produce its first regional earthquake catalog. The stations comprise two permanent (Africa Array and the Malagasy seismic networks) and six temporary seismic networks distributed across the two land masses. We detected and located 178 high-quality events with a magnitude of completeness of M_L3.5, and b-value of 0.76. In the catalog, the events collocate with the known active plate boundaries and associated Quaternary submarine volcanic centers in the Mozambique Channel.

Keywords: Mozambique Channel, Earthquakes, Rift, Earthquake Catalog, Intra-oceanic rifting

1 Introduction

The Mozambique Channel, located between eastern Africa and western Madagascar, constitutes a key tectonic domain within the southwest Indian Ocean, recording both the legacy of Gondwana breakup and ongoing deformation associated with the East African Rift System (EARS) (Reeves and de Wit, 2000; Stamps et al., 2008; Saria et al., 2014; Stamps et al., 2018). Despite its geodynamic importance, seismicity in the Mozambique Channel remains incompletely documented, largely due to the offshore nature of the region and historically sparse seismic station coverage, which has resulted in significant uncertainties in earthquake locations within existing catalogs (Hartnady et al., 1990; Engdahl et al., 1998; Craig et al., 2011). The opening of the Mozambique Channel during the Jurassic-Cretaceous was driven by the separation of Madagascar from the African continent, accompanied by transform faulting and seafloor spreading in the adjacent Mozambique and Somali basins (Malod et al., 1991; Rabinowitz and Woods, 2006). Inherited structures formed during this period, particularly the NNW-SSE-trending Davie Fracture Zone, are widely interpreted as major continent-ocean transform faults and are thought to exert a first-order control on present-day deformation within the channel (Mahanjane, 2014; Franke et al., 2015). More recent tectonic processes related to the southward propagation of the EARS and the development of microplates, including the Rovuma and Lwandle plates, further contribute to the complexity of the regional stress field and plate boundary configuration in southeastern Africa and adjacent offshore regions (Stamps et al., 2008; Saria et al., 2014; Stamps et al., 2021).

Previous studies of seismicity in the Mozambique Channel (Grimison and Chen., 1986; Delavaux and Barth., 2010), have relied on heterogeneous datasets characterized by uneven spatial and temporal coverage, limiting their ability to resolve the geometry and continuity of active structures across the channel (Hartnady et al., 1990; Hartnady, 2002). Deployments of permanent and temporary broadband seismic networks in Madagascar and East Africa, together with the availability of international waveform archives such as IRIS, now provide an opportunity to systematically reassess regional seismicity and improve earthquake locations (Nyblade, 2010; Wysession et al., 2011; Helffrich and Fonseca., 2011; Rümpker, 2015).

In this contribution, we present a revised seismic catalog for the Mozambique Channel covering the period 1989–2021. The catalog is based on waveform data recorded by a dense network of permanent and temporary seismic stations distributed across Madagascar and East Africa and includes rigorously relocated hypocenters using a uniform methodology (Lienert and Havskov, 1995). This revised seismic catalog provides an improved foundation for future investigations of regional tectonics, seismic hazard, and lithospheric structure within the Mozambique Channel and the broader East African plate boundary zone.

2 Regional Tectonics of the Mozambique Channel

The Mozambique Channel, located between eastern Africa and western Madagascar, represents a key tectonic domain within the southwest Indian Ocean, recording both the legacy of Gondwana breakup and ongoing deformation related to the East African Rift System (EARS) (Reeves and de Wit, 2000; Stamps et al., 2008; Saria et al., 2014). The region formed during the Mesozoic breakup of the Gondwana supercontinent, when East Gondwana, including Madagascar and India, separated from the African margin (Konig and Jokat., 2010). Leading to seafloor spreading in the Mozambique and West Somali basins between the Jurassic and Early Cretaceous (180–120 Ma) and establishing the Mozambique Channel as an oceanic corridor between Madagascar and East Africa (Flores , 1971; Malod et al., 1991; Rabinowitz and Woods, 2006; Reeves and de Wit, 2000). This tectonic evolution was accompanied by significant transform faulting, most prominently along the NNW–SSE-trending Davie Fracture Zone (Davie Ridge) (Franke et al., 2015; Fig.1), which is widely interpreted as a continent–ocean transform fault formed during the relative motion between Madagascar and mainland Africa during the Jurassic–Cretaceous (Malod et al., 1991; Rabinowitz and Woods, 2006; Mahanjane, 2014). The Davie Ridge separates crustal domains within the Mozambique Channel and remains a first-order inherited structure influencing later deformation (Klimike and Franke., 2016; Klimike et al, 2016).

In the broader regional framework, the EARS defines the active divergent boundary between the Nubian and Somali plates and has led to the development of several microplates, including the Rovuma and Lwandle plates, within a wide zone of diffuse deformation extending into southeastern Africa and offshore regions (Stamps et al., 2008; Saria et al., 2014, Stamps et al., 2021). Several active or reactivated tectonic boundaries have been proposed within and around the Mozambique Channel, including the NNW-SSE Davie Rift interpreted as the eastern boundary of the Rovuma microplate, an approximately E–W-striking structure in the Comoros region proposed to accommodate deformation between the Somali and Lwandle plates, and a NE–SW-trending structural zone near the Bassas da India–Europa region interpreted as part of the Rovuma–Lwandle plate boundary (Deville et al., 2018, Famin et al., 2020; Stamps et al., 2021; Berthod et al., 2022; Boymond et al., 2025).

The southern Mozambique Channel, particularly the Bassas da India region, has been characterized by clustered seismicity, which has been interpreted as evidence for active deformation along this NE-SW-trending zone (Hartnady et al., 1990; Hartnady, 2002). These observations are consistent with recent bathymetric, volcanic, and seismic studies that document linear volcanic alignments and tectono-magmatic features in the southern channel, suggesting ongoing lithospheric deformation superimposed on inherited Mesozoic structures (Deville et al., 2018; Courgeon et al., 2018; Berthod et al., 2022). Together, these studies highlight the Mozambique Channel as a region where ancient Gondwana breakup structures interact with present-day plate boundary processes, resulting in a complex and spatially distributed pattern of seismicity and deformation (Stamps et al., 2008; Vormann et al., 2020).

3 Data and Methods

3.1 Seismic Station Network

To comprehensively characterize the study area, we use eight seismic networks (figure 2) comprising a total of 266 permanent and temporary stations. These include AFRICAARRAY project (FDSN code: AF, Penn State University 2004), RHUM-RUM project (FDSN code: X1, Rumpker 2015), Seismic Investigations of the Lithospheric Structure of the Tanzanian Craton (FDSN code: XD, Tom Owens and Andy Nyblade 1994), MACOMO project (FDSN code: XV, Wysession et al. 2011), AFRICAARRAY project (FDSN code: YH, Andrew Nyblade 2010) , SEISM project (FDSN code: ZD, Leeds/GFZ Potsdam), MOZART project (FDSN code: 6H, George Helffrich and Fonseca 2011), and the Malagasy seismic networks distributed across the Mozambique Channel. The networks comprise both temporary deployments (X1, XD, XV, YH, ZD, 6H) and permanent stations the Malagasy network, providing a dense spatial and temporal coverage of seismic activity from 1989 to 2021. The combination of broad geographic coverage and high station density on both sides of the Mozambique Channel is critical for accurate event detection, location. Detailed lists of all stations included in this study, separated by Malagasy and East African locations, are provided in the supplementary material.

3.2 Data processing and Catalog development

Data acquisition was performed in three successive stages to ensure consistent waveform coverage across the Mozambique Channel. First, we compile a reference seismic catalog from the National Data Center for Seismic and Infrasonic in Madagascar (NDC-Madagascar), Institute and Observatory of Geophysics in Antananarivo (IOGA). This catalog includes 178 seismic events recorded between 1990 and 2021 using only seismic stations located in Madagascar. For these events, waveform data were available in a different format but converted into the common MiniSEED format to ease the computation. In the second stage,we submit the same event catalog to the IRIS (Incorporated Research Institutions for Seismology) Data Management Center to retrieve waveforms recorded from seismic stations located in East African countries bordering the Mozambique Channel, including Mozambique, Tanzania, Malawi, and South Africa. While requesting for waveforms for each station, the start time was computed from event origin time with respect to the epicentral distance from each event location. For each event, waveform length was extended by 1200 s to ensure sufficient waveform duration for signal analysis and to match the time window of the waveforms recorded by Malagasy stations. Data retrieval was carried out through automated requests to the IRIS archive and other available databases. For the third and final stage we merge waveform datasets recorded by seismic stations in Madagascar with those obtained from East African stations. All waveforms were standardized and stored in MiniSEED format, then we imported into the event location and processing software to form a unified dataset suitable for hypocentral location and subsequent seismic analyses.

3.3 Event location

For each event, four parameters were determined: origin time, hypocenter coordinates (latitude and longitude), focal depth, and magnitude. We perform event location using the Fortran-based program HYP, implemented within the SEISAN software package. HYP is an enhanced version of the HYPOCENTER algorithm developed by Lienert and Havskov (1995), designed to iteratively refine hypocenter positions using travel-time data. The location procedure employed an iterative inversion of P- and S-wave arrival times. For each event, HYP calculates partial derivatives of observed arrival times with respect to hypocentral parameters and minimizes residuals between observed and predicted travel times. Input data included the initial catalog locations, precise station coordinates, and a 1D seismic velocity model. The AK135 global velocity model (Kennett et al., 1995) was used because no regional velocity model is currently available for the Mozambique Channel. The program outputs updated hypocentral parameters and the associated root mean square (RMS) travel-time residual, which serves as a quantitative measure of location quality. To further reduce residuals and improve accuracy, phase picking was carefully refined for each event through iterative adjustment of P- and S-wave arrivals. The combination of high station density and broadband waveform data maximized the robustness and precision of the located catalog, producing a consistently improved dataset suitable for subsequent seismic analyses.

4 Results

4.1 Event distribution and statistics

Between 1990 and 2021, we detected and located 178 high-quality events. All events were initially located using the seismic network configuration, and was performed using the HYP program, with preferred solutions selected based on the minimization of root mean square (RMS) travel-time residuals. The spatial distribution of the hypocenters shows a defined clustering along the axis of the Mozambique Channel. The clusters continue south-southeastwards from the northwestern Mozambique coastal margin (10.85°S, 40.62°E), to the western coastal areas of southern Madagascar (24.64°S and 43.30°E). The events appear to be concentrated within a narrow corridor, forming a continuous NNW–SSE-oriented zone of seismicity between the eastern African margin and the southwestern margin of Madagascar. The persistence of this spatial pattern throughout the seismicity record period highlights the tectonic origin of the observed seismicity. The frequency-magnitude distribution of the catalog (Figure 4) produced a b-value of 0.76, suggesting a predominance of relatively larger magnitude events in the catalog compared to smaller ones. The cumulative distribution closely follows the Gutenberg Richter law for M≥3.5, indicating that the magnitude of completeness of the catalog (Mc) is M3.5. The cumulative distribution shows the actual frequency of events per magnitude bin, confirming that the majority of events are clustered around moderate magnitudes (M3 – 4), while large events (M>5) are rare.

The horizontal errors in the locations of the events are 0 - 46 km in E-W direction and 0 - 48 km in N-S direction. Most of the events are in the crust (<60 km), however, some outlier events appear deeper but have much larger depth uncertainties

5 Synthesis

We present here a new seismic catalog for the Mozambique Channel that comprises high-quality manual event detections based on >9 station detections in mainland eastern Africa and Madagascar (Fig. 3a, 5a). The catalog has a Mc of M3.5, suggesting that the microseismic events are not captured in the catalog, likely due to the large distance of the stations used for event detection. However, the detected and located events colocate with known active plate boundaries in the Mozambique Channel, and primarily along the bathymetric trace of the NNW-SSE striking Davie Rift (Fig. 3). More broadly, the detected events only occur along the northern and central segments of the Davie Rift, and more sparsely in the southern segment. Although our catalog detected more events in the southern Davie Rift than global catalogs (Fig. 1b), the rift segment remains relatively seismically quiet. We interpret that the consistency of seismicity sparseness of the southern Davie Rift across the different seismic catalogs suggest that active deformation in this rift segment may be aseismic, or that there is significant strain accumulation on the active faults in the rift segment. Away from the Davie Rift, several of the events occur in the Zambezi Basin, defining a NE-SW trend that splay southwestward from the Davie Rift towards the Mozambique coastal margin, which we interpret to be associated with the Rovuma-Lwandle plate boundary (see Fig. 1a). Furthermore, a few of the events are colocated with the Comoros volcanic island chain which defines an active tectonic plate boundary along the southwestern boundary of the Somalian Plate.

6 Uncertainties

Hypocentral locations and associated uncertainties depend strongly on the assumed velocity model and the geometry of the seismic network. In this study, the global one-dimensional AK135 velocity model was used for all events. Although AK135 provides a stable and internally consistent reference model, it does not fully represent the complex crustal and upper-mantle structure of the Mozambique Channel. As a result, earthquake depths are generally less well constrained than epicentral locations, as reflected by large depth uncertainties. The mean location uncertainties are approximately ~15.70 km N-S, ~16.45 km E-W, and ~22.74 km in depth, with the larger depth errors primarily attributed to limitations of the global velocity model rather than station coverage, which is relatively good on both sides of the channel. In the absence of any local or regional velocity models for the Mozambique Channel, AK135 represents the most appropriate available choice. The use of a single velocity model ensures internal consistency across the dataset, and the reported uncertainties primarily reflect relative location errors rather than absolute mislocations. Within these constraints, the colocation of the earthquakes with known active plate boundaries suggests that within the extents of the stated location uncertainties, the catalog is useful for first-order investigations of tectonic deformation at a regional scale. Future work to advance the catalog should include event location tests using a variety of available crustal and lithospheric velocity models with an assessment and comparison of the resulting location error distributions. Furthermore, a relative relocation approach that is compatible with large inter-station distances may provide a reduced uncertainty in the event locations.

Conclusions

We present a first regional seismic catalog for the Mozambique Channel, using a combination of seismic station networks on mainland eastern Africa, and Madagascar island. We detected and located 178 of high-quality events with a magnitude of completeness of M_L3.5, and b-value of 0.76. The uncertainties in the event location generally range 0 - 48 km, given the large station distances. However, the events collocate with the known active plate boundaries and associated Quaternary submarine volcanic centers in the Mozambique Channel. The presented seismic catalog is preliminary but provides a useful framework for future investigations of seismicity and the associated tectonics of the Mozambique Channel.

Acknowledgements

This project is funded by the National Science Foundation (NSF) Grant #2501725 awarded to Folarin Kolawole

Open Research

The earthquake waveform datasets supporting this study are publicly accessible through the EarthScope Consortium Web Services. The earthquake catalog developed in the study is provided as a table (Table 1) in the manuscript.

Conflict of Interest Statement

The authors have no conflicts of interest to disclose.

References

Andrew Nyblade. (2010). AfricaArray SE Tanzania Basin Experiment [Data set]. International Federation of Digital Seismograph Networks. https://doi.org/10.7914/SN/YH_2010

Berthod, C., Bachèlery, P., Jorry, S. J., Pitel-Roudaut, M., Ruffet, G., Revillon, S., ... & Doucelance, R. (2022). First characterization of the volcanism in the southern Mozambique Channel: Geomorphological and structural analyses. *Marine Geology*, *445*, 106755.https://doi.org/10.1016/j.margeo.2022.106755

Boymond, P., Feuillet, N., Thinon, I., Scholtes, L., Zaragosi, S., Leroy, S., & Lemoine, A. (2025). En-échelon rifting and origin of the volcanism in the Comoros. *Geochemistry, Geophysics, Geosystems*, *26*(2), e2024GC011576. https://doi.org/10.1029/2024GC011576

Courgeon, S., Bachèlery, P., Jouet, G., Jorry, S. J., Bou, E., BouDagher-Fadel, M. K., ... & Poli, E. (2018). The offshore east African rift system: new insights from the Sakalaves seamounts (Davie Ridge, SW Indian Ocean). *Terra Nova*, *30*(5), 380-388. https://doi.org/10.1111/ter.12353

Craig, T. J., Jackson, J. A., Priestley, K., & McKenzie, D. (2011). Earthquake distribution patterns in Africa: Their relationship to variations in lithospheric and geological structure, and their rheological implications. *Geophysical Journal International*, *185*(1), 403-434.https://doi.org/10.1111/j.1365-246X.2011.04950.x

Delvaux, D., & Barth, A. (2010). African stress pattern from formal inversion of focal mechanism data. *Tectonophysics*, *482*(1-4), 105-128.https://doi.org/10.1016/j.tecto.2009.05.009

Deville, E., Marsset, T., Courgeon, S., Jatiault, R., Ponte, J. P., Thereau, E., ... & Droz, L. (2018). Active fault system across the oceanic lithosphere of the Mozambique Channel: Implications for the Nubia–Somalia southern plate boundary. *Earth and Planetary Science Letters*, *502*, 210-220.https://doi.org/10.1016/j.epsl.2018.08.052

Famin, V., Michon, L., & Bourhane, A. (2020). The Comoros archipelago: a right-lateral transform boundary between the Somalia and Lwandle plates. *Tectonophysics*, *789*, 228539.https://doi.org/10.1016/j.tecto.2020.228539

Franke, D., Jokat, W., Ladage, S., Stollhofen, H., Klimke, J., Lutz, R., ... & Schreckenberger, B. (2015). The offshore East African Rift System: Structural framework at the toe of a juvenile rift. *Tectonics*, *34*(10), 2086-2104. https://doi.org/10.1002/2015TC003922

Flores, G. (1971). Suggested origin of the Mozambique Channel. *South African Journal of Geology*, *74*(2), 109-110.https://journals.co.za/doi/pdf/10.10520/AJA10120750_328

George Helffrich & Fonseca, J F B D. (2011). Mozambique Rift Tomography [Data set]. International Federation of Digital Seismograph Networks. https://doi.org/10.7914/SN/6H_2011

Grimison, N. L., & Chen, W. P. (1988). Earthquakes in the Davie Ridge-Madagascar region and the southern Nubian-Somalian plate boundary. *Journal of Geophysical Research: Solid Earth*, *93*(B9), 10439-10450.https://doi.org/10.1029/JB093iB09p10439

Hartnady, C. J. H., Joubert, P., & Stettler, E. (1990). Seismicity and plate boundary evolution in southeastern Africa. *Tectonophysics*, **212**, 89–98.Online ISSN 1996-8590 ISSN 1012-0750

Hartnady, C. J. H. (2002). Earthquake hazard in Africa : perspectives on the Nubia-Somalia boundary : news and view.https://hdl.handle.net/10520/EJC97553

Kennett, B. L., Engdahl, E. R., & Buland, R. (1995). Constraints on seismic velocities in the Earth from traveltimes. *Geophysical Journal International*, *122*(1), 108-124.https://doi.org/10.1111/j.1365-246X.1995.tb03540.x

Klimke, J., & Franke, D. (2016). Gondwana breakup: no evidence for a Davie Fracture Zone offshore northern Mozambique, Tanzania and Kenya. *Terra Nova*, *28*(4), 233-244.https://doi.org/10.1111/ter.12214

Klimke, J., Franke, D., Gaedicke, C., Schreckenberger, B., Schnabel, M., Stollhofen, H., ... & Chaheire, M. (2016). How to identify oceanic crust—Evidence for a complex break-up in the Mozambique Channel, off East Africa. *Tectonophysics*, *693*, 436-452.https://doi.org/10.1016/j.tecto.2015.10.012Get rights and content

König, M., & Jokat, W. (2010). Advanced insights into magmatism and volcanism of the Mozambique Ridge and Mozambique Basin in the view of new potential field data. *Geophysical Journal International*, *180*(1), 158-180.https://doi.org/10.1111/j.1365-246X.2009.04433.x

Lienert, B. R., & Havskov, J. (1995). A computer program for locating earthquakes both locally and globally. *Seismological Research Letters*, **66**, 26–36. https://doi.org/10.1785/gssrl.66.5.26

Mahanjane, E. S. (2014). The Davie Fracture Zone and adjacent basins in the Mozambique Channel: A new geological interpretation. *Marine and Petroleum Geology*, **57**, 581–596.https://doi.org/10.1016/j.marpetgeo.2014.06.015

Malod, J. A., Mougenot, D., Raillard, S., & Maillard, A. (1991). The Davie Ridge, Mozambique Channel: Crustal structure and origin. *Tectonophysics*, **191**, 1–26.

Penn State University, 2004. AfricaArray. International Federation of Digital Seismograph Networks, Other/Seismic Network. doi:10.7914/SN/AF.

Rabinowitz, P. D., & Woods, S. (2006). The Africa–Madagascar connection and mammalian migrations. *Journal of African Earth Sciences*, *44*(3), 270-276.https://doi.org/10.1016/j.jafrearsci.2005.12.005

Reeves, C., & de Wit, M. (2000). Making ends meet in Gondwana: Retracing the transforms of the Indian Ocean and reconnecting continental shear zones. *Terra Nova*, **12**, 272–280. https://doi.org/10.1046/j.1365-3121.2000.00309.x

Rümpker, G. (2015). RHUM-RUM Seychelles [Data set]. GFZ Data Services. https://doi.org/10.14470/K67568473685

Saria, E., Calais, E., Stamps, D. S., Delvaux, D., & Hartnady, C. (2014). Present-day kinematics of the East African Rift. *Journal of Geophysical Research: Solid Earth*, **119**, 3584–3600. https://doi.org/10.1002/2013JB010901

Stamps, D. S., Calais, E., Saria, E., Hartnady, C., Nocquet, J. M., Ebinger, C., & Fernandes, R. (2008). A kinematic model for the East African Rift. *Geophysical Research Letters*, **35**, L05304. https://doi.org/10.1029/2007GL032781

Stamps, D. S., Saria, E., & Kreemer, C. (2018). A geodetic strain rate model for the East African Rift System. *Scientific reports*, *8*(1), 732.https://doi.org/10.1038/s41598-017-19097-w

Stamps, D. S., Kreemer, C., Fernandes, R., Rajaonarison, T. A., & Rambolamanana, G. (2021). Redefining east African rift system kinematics. *Geology*, *49*(2), 150-155.https://doi.org/10.1130/G47985.1

Thinon, I., Lemoine, A., Leroy, S., Paquet, F., Berthod, C., Zaragosi, S., ... & Sadeski, L. (2022). Volcanism and tectonics unveiled in the Comoros Archipelago between Africa and Madagascar. *Comptes Rendus. Géoscience*, *354*(S2), 7-34.10.5802/crgeos.159

Tom Owens & Andy Nyblade. (1994). Seismic investigations of the Lithospheric Structure of the Tanzanian Craton [Data set]. International Federation of Digital Seismograph Networks. https://doi.org/10.7914/SN/XD_1994

Vormann, M., & Jokat, W. (2021). Crustal variability along the rifted/sheared East African margin: a review. *Geo-Marine Letters*, *41*(2), 19.https://doi.org/10.1007/s00367-021-00690-y

Wysession, M., Wiens, D. & Nyblade, A., 2011. Investigation of Sources of Intraplate Volcanism Using PASSCAL Broadband Instruments in Madagascar, the Comores, and Mozambique, International Federation of Digital Seismograph Networks. Other/Seismic Network. doi:10.7914/SN/XV_2011.

Figures

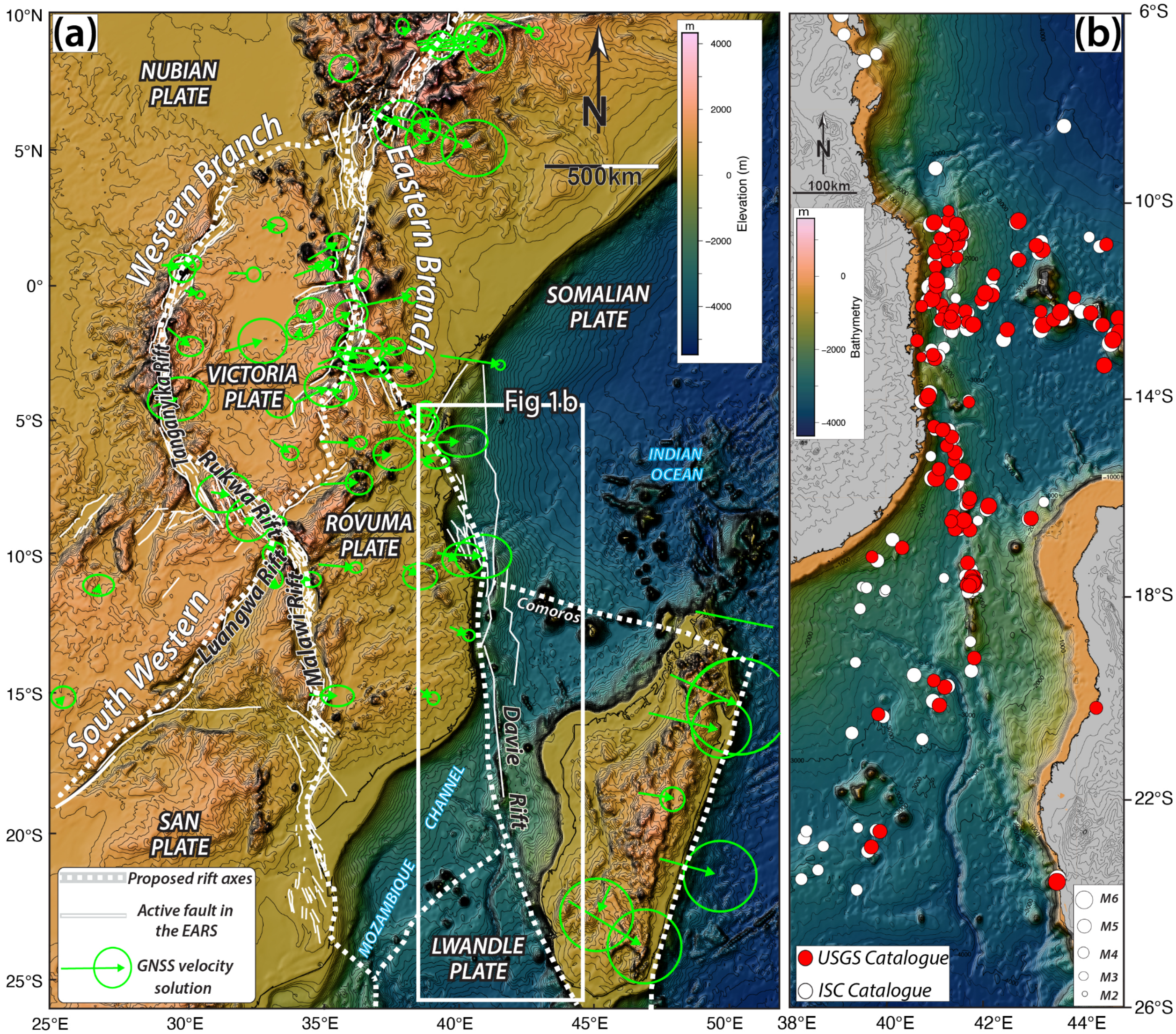

Figure 1:(a) Tectonic framework of the East African Rift System, illustrating GPS velocity vectors (after Saria et al., 2014; Stamps et al., 2018), plate boundaries (after Stamps et al., 2021 and Wedmore et al., 2021), and active faults (after Styron and Pagani, 2020). **(b)** Seismicity of the Mozambique Channel 1989-2021 from USGS catalog in red and ISC catalog in white.

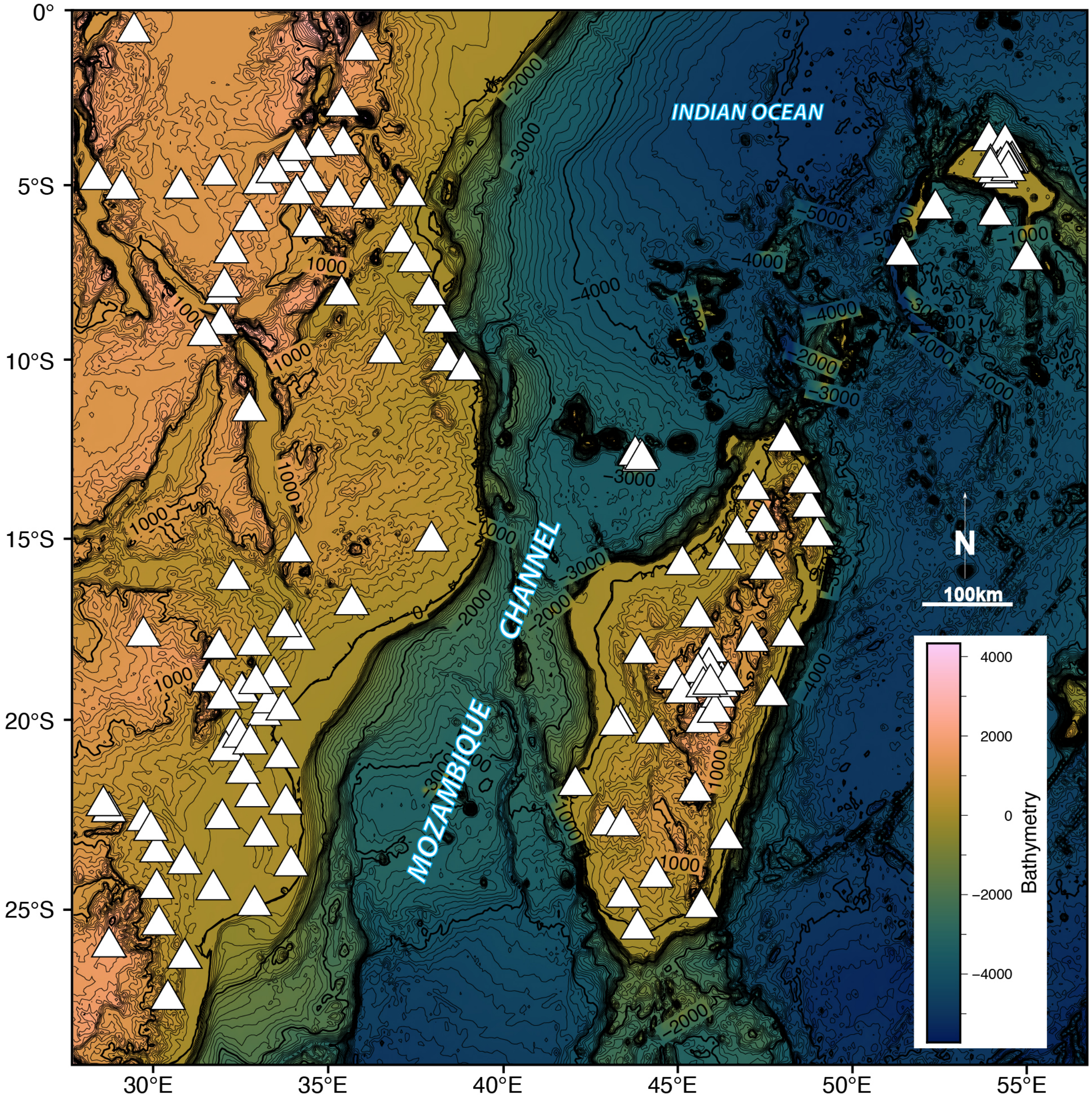

Figure 2: Spatial distribution of seismic stations used in this study, comprising stations in mainland eastern Africa and in Madagascar.

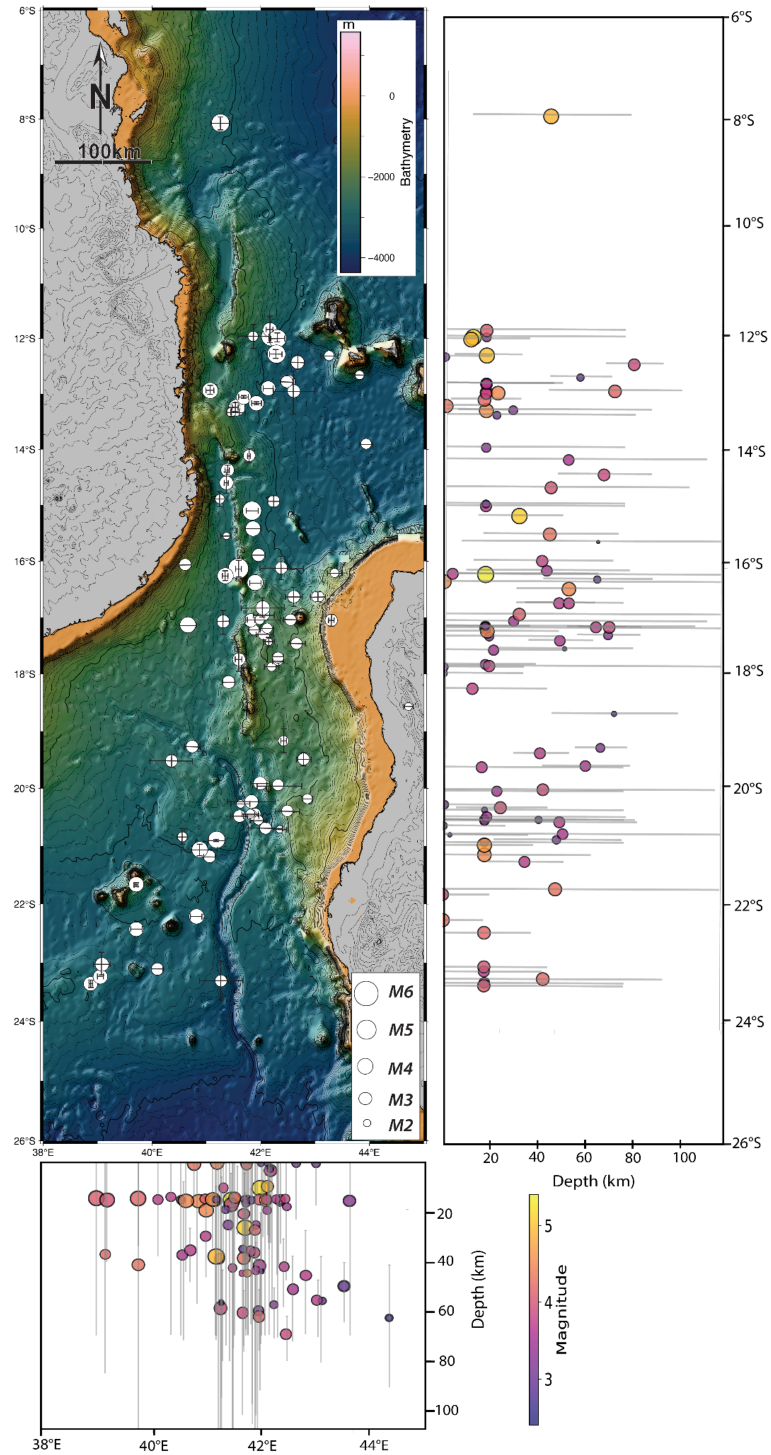

Figure 3: Spatial distribution of seismic events located in this study overlaid with location uncertainties in xy-direction (in map), and depth uncertainties in cross-sections. The cross-sections are projected along a central longitude 41°E (right panel) and along a central latitude 16°S (bottom panel). Note that we exclude events located at >70 km depths as they have large (>50 km) location uncertainties.

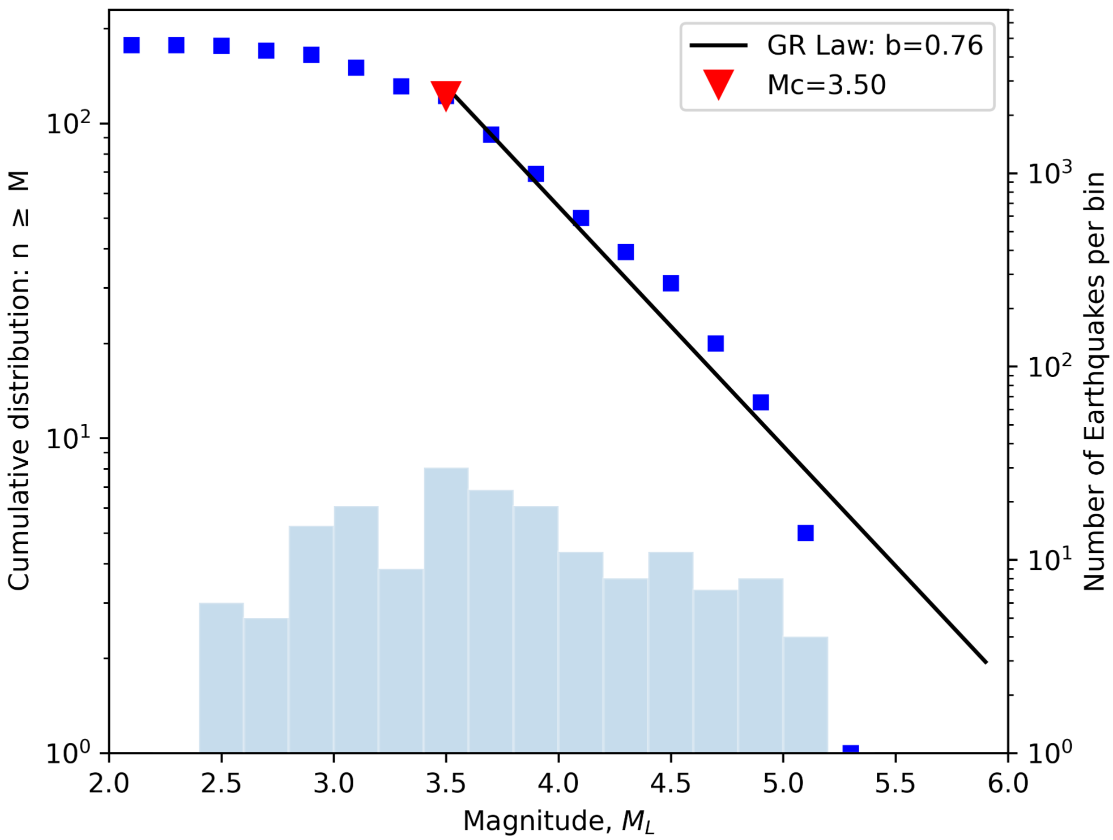

Figure 4: Frequency–magnitude distribution of events in the catalog, showing a b−value of 0.76. Only events with magnitudes ≥ $M_{(c)}$ are included in the Gutenberg–Richter fit.

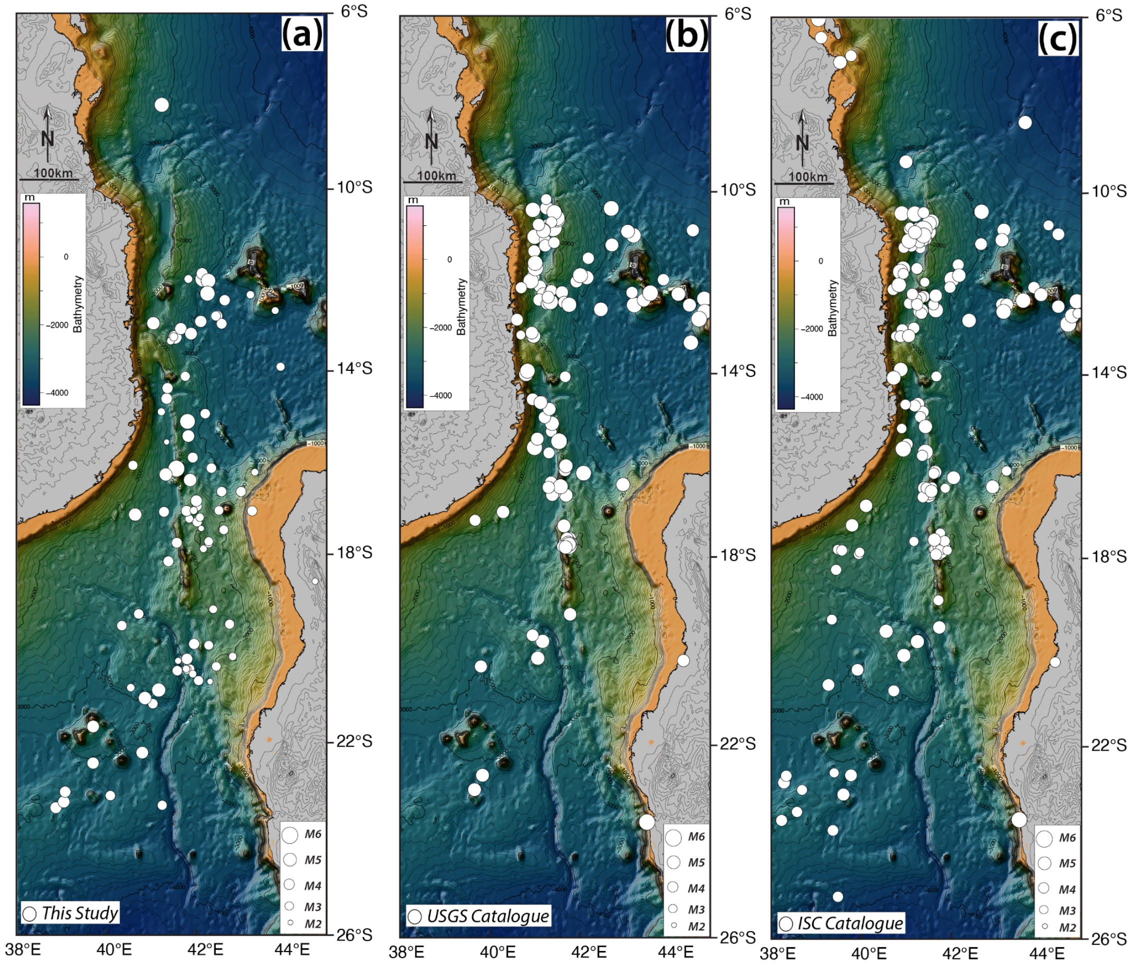

Figure 5: Spatial distribution of events in the seismic catalog from **(a)** this study (excluding events with >50 km location uncertainties), **(b)** public domain catalog from USGS, and **(c)** public domain catalog from ISC.

Table 1: List of events detected and located in this study

Date	Time	latitude	longitude	depth	mag	erlat	erlon	erdepth	erlat_deg	erlon_deg
21/10/1992	21:32:11.760	-17.3	42.62	230.5	2.8	18.98	41.9	77.8	0.17	0.4
22/07/1994	19:54:36.650	-11.09	40.72	71.9	3.7	48.32	57.1	238.3	0.44	0.52
19/08/1994	05:50:47.260	-12.6	41.48	79.4	4.3	97.44	114.7	100.6	0.88	1.06
03/10/1994	01:46:03.360	-12.92	41.37	77.5	3.6	83.03	110.6	226.9	0.75	1.02
04/02/1995	20:41:17.870	-10.26	40.29	15.0	3.7	614.87	788.5	25.22	5.54	7.22
08/06/1995	16:11:58.590	-13.24	41.53	24.7	3.2	8.88	8.8	50.0	0.08	0.08
12/06/1995	19:49:50.100	-13.33	41.46	18.8	3.0	15.16	17.3	50.0	0.14	0.16
17/06/1995	22:24:09.200	-14.89	41.25	15.0	3.0	24.02	13.8	50.0	0.22	0.13
24/06/1995	17:38:20.670	-12.9	42.14	61.4	4.2	0.0	10.34	24.26	0.0	0.1
20/07/1995	05:08:33.420	-13.17	41.92	0.6	4.3	0.0	14.95	12.39	0.0	0.14
10/08/1995	00:41:16.000	-16.38	41.9	45.1	4.5	0.0	11.22	19.44	0.0	0.11
21/08/1995	22:08:30.490	-20.71	42.35	2.5	2.5	0.0	14.4	27.74	0.0	0.14
27/09/1995	11:05:35.080	-15.55	41.37	55.6	2.4	14.02	10.3	50.0	0.13	0.1
04/10/1995	23:19:42.220	-11.88	42.12	76.9	3.0	0.0	16.84	22.75	0.0	0.16
17/10/1995	20:05:32.470	-17.15	41.83	3.6	2.6	39.16	53.5	53.0	0.35	0.5
22/08/1996	07:14:56.310	-14.93	42.24	15.0	3.7	15.19	12.7	50.0	0.14	0.12
27/08/1996	20:29:40.600	-17.43	42.15	43.6	2.5	0.0	10.98	24.59	0.0	0.1
04/05/1998	07:04:37.120	-17.04	41.98	15.0	3.0	34.33	33.4	75.8	0.31	0.31
26/10/1998	08:46:13.160	-20.44	41.81	34.5	2.9	20.46	16.2	34.6	0.18	0.16
17/06/2000	07:39:26.230	-20.25	42.28	321.1	2.6	62.09	138.3	192.6	0.56	1.33
29/06/2000	23:29:32.410	-16.63	43.05	45.1	3.7	23.38	15.4	19.5	0.21	0.14
06/07/2000	03:53:42.560	-24.11	40.37	78.8	3.8	0.0	13.05	16.5	0.0	0.13
11/09/2000	02:52:17.220	-12.31	43.26	0.1	3.1	0.0	18.08	16.22	0.0	0.17
03/10/2000	01:24:33.870	-17.25	42.13	15.0	3.0	43.32	70.8	95.8	0.39	0.67
21/10/2000	02:12:08.590	-19.01	42.62	188.7	3.1	19.66	33.8	91.4	0.18	0.32
03/11/2000	20:23:40.490	-12.66	43.82	48.9	2.9	0.0	19.66	11.27	0.0	0.18
20/11/2000	22:32:11.930	-20.23	41.83	20.7	4.0	22.11	46.4	16.62	0.2	0.45

11/09/2001	01:12:16.780	-23.03	39.08	15.0	4.0	0.0	19.49	22.47	0.0	0.19
03/10/2001	22:42:56.510	-11.8	41.48	140.9	3.9	18.49	16.58	21.37	0.17	0.15
07/10/2001	23:33:43.400	-19.59	42.69	126.5	4.3	13.25	17.46	22.99	0.12	0.17
27/10/2001	01:50:46.200	-23.06	41.33	77.7	3.5	12.24	17.12	14.74	0.11	0.17
28/11/2001	03:18:14.720	-12.8	42.02	74.2	4.8	15.49	16.92	23.04	0.14	0.16
09/12/2001	09:22:35.300	-13.4	41.73	206.1	5.2	16.64	10.05	13.22	0.15	0.09
15/12/2001	06:16:25.970	-12.78	42.48	15.0	3.6	0.0	10.65	27.26	0.0	0.1
16/12/2001	10:46:37.830	-13.36	41.16	75.8	4.5	16.06	10.09	12.03	0.14	0.09
16/01/2002	23:57:25.520	-16.83	42.04	27.2	4.1	45.16	43.5	110.3	0.41	0.41
09/04/2002	01:11:23.480	-12.95	42.61	14.9	3.8	44.66	41.4	0.0	0.4	0.38
06/05/2002	06:30:30.700	-24.6	41.98	76.5	4.1	10.84	11.62	27.97	0.1	0.12
13/06/2002	05:37:06.350	-18.69	40.99	75.3	3.9	18.87	17.8	22.84	0.17	0.17
16/06/2002	03:00:36.690	-17.28	40.67	76.9	3.6	13.49	17.26	27.94	0.12	0.16
16/07/2002	14:50:27.320	-12.28	42.29	15.1	5.0	0.0	11.71	12.32	0.0	0.11
25/07/2002	08:48:21.600	-11.93	41.45	77.7	4.6	19.0	16.33	16.78	0.17	0.15
04/08/2002	11:31:37.960	-17.35	42.25	21.5	4.1	68.48	30.1	29.3	0.62	0.28
16/09/2002	14:49:12.810	-20.89	41.19	15.0	4.7	0.0	16.08	17.17	0.0	0.16
14/10/2002	19:54:59.760	-16.63	42.61	41.6	3.7	20.21	17.6	12.8	0.18	0.17
26/10/2002	09:49:49.570	-13.41	41.29	78.3	3.8	12.42	10.93	27.94	0.11	0.1
08/11/2002	05:04:40.330	-17.05	41.82	59.7	3.9	0.0	10.46	11.48	0.0	0.1
15/11/2002	08:27:12.260	-21.13	40.17	77.9	4.9	18.17	15.55	20.59	0.16	0.15
14/12/2002	14:21:22.670	-17.36	42.93	189.8	3.6	18.77	12.58	23.2	0.17	0.12
24/12/2002	02:18:10.640	-17.13	40.66	15.7	4.5	0.0	15.92	25.43	0.0	0.15
02/01/2003	16:04:43.520	-15.71	42.01	3.4	3.9	19.58	127.0	122.5	0.18	1.19
06/01/2003	02:15:57.870	-15.42	41.86	38.1	4.3	0.0	15.14	24.58	0.0	0.14
03/02/2003	19:54:50.390	-15.49	41.84	11.9	4.0	14.27	84.2	79.9	0.13	0.79
18/04/2003	00:27:04.900	-12.78	42.51	15.0	3.9	0.0	12.0	24.14	0.0	0.11
18/05/2003	23:08:11.070	-17.46	42.66	18.0	3.5	0.0	17.85	26.31	0.0	0.17
28/05/2003	12:33:49.130	-19.27	40.74	34.9	3.7	0.0	14.56	10.11	0.0	0.14

01/06/2003	22:29:49.390	-22.21	40.82	0.1	4.3	0.0	13.66	13.97	0.0	0.13
29/07/2003	01:29:27.460	-15.89	41.96	35.4	3.8	0.0	12.92	25.44	0.0	0.12
10/08/2003	23:56:28.530	-20.84	40.56	15.0	3.1	21.89	9.6	50.0	0.2	0.09
17/08/2003	12:12:08.750	-16.06	40.61	37.1	3.6	0.0	11.39	29.74	0.0	0.11
18/08/2003	11:15:33.740	-17.19	42.12	59.3	3.2	0.0	16.12	11.49	0.0	0.15
26/08/2003	12:16:53.750	-17.22	41.88	16.4	3.2	0.0	12.91	26.04	0.0	0.12
01/09/2003	02:07:08.030	-13.06	41.69	14.3	4.2	0.0	14.32	12.82	0.0	0.13
21/09/2003	20:41:26.570	-20.39	42.49	15.8	3.5	47.95	24.4	50.0	0.43	0.23
09/10/2003	03:16:46.110	-16.95	42.06	25.2	3.5	28.11	33.2	69.8	0.25	0.31
19/10/2003	01:50:58.520	-12.0	42.31	9.4	4.9	0.0	15.25	20.85	0.0	0.14
23/11/2003	20:01:01.620	-17.04	42.55	15.0	3.5	0.0	13.04	15.62	0.0	0.12
01/12/2003	04:31:48.780	-16.12	42.38	3.1	3.7	34.24	43.3	52.2	0.31	0.41
05/12/2003	05:25:31.940	-20.3	41.52	31.8	5.0	130.88	129.9	254.1	1.18	1.25
17/07/2012	10:13:45.910	-20.84	40.97	172.6	3.7	13.41	11.13	28.49	0.12	0.11
12/08/2012	19:11:13.600	-14.58	41.25	234.8	4.0	20.25	4.3	29.5	0.18	0.04
13/08/2012	04:14:05.470	-14.37	41.39	57.6	3.9	20.94	5.3	17.14	0.19	0.05
28/08/2012	16:07:53.640	-11.84	42.17	15.0	4.1	28.7	4.8	50.0	0.26	0.04
07/11/2012	11:26:14.730	-16.26	41.35	0.1	4.5	17.82	6.0	193.2	0.16	0.06
08/11/2012	10:21:40.650	-17.74	41.6	16.4	3.8	29.1	7.3	144.2	0.26	0.07
13/11/2012	17:19:58.570	-16.98	44.23	15.0	2.9	69.05	11.5	50.0	0.62	0.11
19/11/2012	00:37:55.670	-14.6	41.37	38.5	4.0	21.15	4.4	50.0	0.19	0.04
29/11/2012	02:41:59.880	-17.07	41.31	15.0	3.8	33.65	11.0	343.8	0.3	0.1
14/12/2012	15:18:46.040	-16.13	41.59	15.0	5.4	9.7	5.4	142.7	0.09	0.05
18/12/2012	17:39:40.520	-14.11	41.79	44.8	3.6	13.39	2.4	50.0	0.12	0.02
08/03/2013	15:23:47.380	-23.24	39.05	36.3	4.2	25.52	9.4	43.0	0.23	0.09
20/03/2013	05:21:53.630	-11.96	42.19	10.2	5.2	9.65	3.6	0.0	0.09	0.03
03/05/2013	09:58:25.980	-18.14	41.41	10.4	3.8	0.0	11.83	26.57	0.0	0.11
05/05/2013	12:12:05.990	-23.36	38.87	15.0	4.1	6.74	1.9	50.0	0.06	0.02
06/06/2013	09:37:27.860	-16.43	41.43	165.2	4.4	18.91	8.9	79.2	0.17	0.08

20/06/2013	05:47:41.770	-21.66	39.71	40.6	4.3	8.41	4.2	59.2	0.08	0.04
09/08/2013	19:23:23.160	-12.94	41.07	19.2	4.5	14.45	5.6	0.0	0.13	0.05
11/08/2013	06:48:18.680	-12.93	41.09	15.0	4.1	7.45	2.3	0.0	0.07	0.02
12/08/2013	21:58:14.460	-12.43	42.76	75.9	3.8	16.45	11.74	23.82	0.15	0.11
13/08/2013	01:29:39.650	-23.83	39.64	147.1	4.0	5.85	2.6	48.9	0.05	0.03
12/11/2013	12:25:14.540	-15.1	41.84	27.1	5.1	0.0	11.82	15.43	0.0	0.11
03/02/2018	05:51:04.890	-17.71	42.32	15.0	3.4	0.0	12.12	17.77	0.0	0.11
04/02/2018	12:09:13.340	-22.43	39.71	15.0	4.2	0.0	18.32	16.51	0.0	0.18
08/03/2018	08:50:06.640	-17.81	37.24	15.1	5.0	246.34	841.9	61.3	2.22	7.97
17/04/2018	04:04:45.400	-19.05	40.48	0.01	3.9	138.9	98.7	120.1	1.25	0.94
10/07/2018	23:45:28.780	-21.75	41.77	223.4	4.2	10.17	15.12	14.53	0.09	0.15
16/07/2018	01:11:22.950	-21.07	41.85	98.8	4.9	10.41	15.91	23.55	0.09	0.15
29/07/2018	08:58:24.250	-15.02	43.26	19.2	3.6	46.18	136.5	121.0	0.42	1.27
29/07/2018	12:33:07.300	-16.68	41.77	145.8	3.2	18.35	13.21	13.73	0.17	0.12
20/11/2018	19:33:32.390	-13.25	41.56	15.0	4.6	0.0	19.7	10.9	0.0	0.18
21/02/2019	09:37:17.290	-21.06	40.88	15.0	4.5	16.91	34.7	38.1	0.15	0.33
13/04/2019	09:21:04.460	-19.94	42.32	19.4	3.5	14.04	41.7	45.5	0.13	0.4
13/05/2019	14:59:45.000	-19.92	41.02	0.01	4.7	22.66	53.5	57.4	0.2	0.51
13/05/2019	14:59:45.000	-19.8	41.2	160.1	4.0	13.87	19.37	12.75	0.12	0.19
31/07/2019	08:18:58.550	-23.84	40.42	77.6	4.0	16.34	15.36	11.81	0.15	0.15
08/10/2019	21:50:17.890	-12.09	43.11	76.7	4.5	17.28	13.68	22.65	0.16	0.13
08/10/2019	21:50:21.550	-13.08	42.03	167.6	4.4	16.72	17.62	14.75	0.15	0.16
14/10/2019	18:16:56.610	-17.8	42.16	22.1	3.4	200.55	754.5	55.1	1.81	7.14
30/10/2019	16:21:58.100	-13.66	46.05	249.2	3.5	14.89	19.86	14.84	0.13	0.18
20/11/2019	18:33:19.680	-17.57	42.17	15.6	3.6	45.16	61.5	83.8	0.41	0.58
21/11/2019	02:39:10.170	-18.01	40.57	0.2	3.3	38.61	61.6	67.7	0.35	0.58
04/12/2019	11:58:34.250	-17.34	42.42	0.01	3.6	261.5	965.1	13.92	2.36	9.11
11/03/2020	22:09:16.130	-20.22	41.96	15.0	3.6	40.29	252.0	301.4	0.36	2.42
18/03/2020	22:06:58.080	-15.68	41.86	18.9	3.6	36.46	104.1	96.4	0.33	0.97

01/04/2020	22:18:21.990	-13.7	41.38	76.5	4.8	656.09	598.7	11.77	5.91	5.55
25/04/2020	03:52:25.600	-20.35	40.78	163.0	4.7	19.08	12.4	12.9	0.17	0.12
01/05/2020	23:20:34.340	-17.76	42.32	0.1	3.1	0.0	10.21	28.44	0.0	0.1
16/05/2020	16:49:10.550	-20.82	41.29	260.1	3.2	15.03	10.51	15.57	0.14	0.1
17/05/2020	08:14:38.590	-20.55	41.96	0.1	3.0	0.0	17.08	21.96	0.0	0.16
29/05/2020	21:51:14.730	-16.35	41.93	262.5	3.0	12.85	10.37	22.19	0.12	0.1
11/06/2020	14:52:03.650	-16.95	42.08	22.1	3.3	98.68	121.6	293.2	0.89	1.15
14/06/2020	01:25:19.240	-16.89	42.14	0.1	3.5	46.95	64.9	84.3	0.42	0.61
30/06/2020	21:54:24.690	-19.49	42.79	51.3	3.6	12.52	14.97	16.02	0.11	0.14
05/08/2020	03:02:04.070	-11.57	42.05	263.3	3.9	13.64	19.72	29.25	0.12	0.18
11/08/2020	05:10:27.190	-14.58	41.0	75.5	5.2	13.23	15.19	24.06	0.12	0.14
12/08/2020	17:13:31.470	-8.07	41.26	37.9	4.9	11.2	13.38	28.86	0.1	0.12
12/08/2020	18:01:45.640	-7.59	41.61	78.5	5.0	15.11	14.17	14.44	0.14	0.13
13/08/2020	14:55:09.890	-8.36	40.74	38.9	4.7	620.89	272.6	27.9	5.59	2.48
13/08/2020	14:55:13.730	-8.29	41.78	15.0	4.5	56.58	97.7	50.0	0.51	0.89
20/08/2020	08:58:04.050	-11.96	41.86	15.0	3.2	24.56	31.7	50.0	0.22	0.29
18/09/2020	05:39:43.110	-21.65	40.81	11.1	3.4	64.81	181.9	213.5	0.58	1.76
21/09/2020	04:11:21.150	-20.48	41.61	42.0	3.7	29.41	18.6	27.9	0.26	0.18
21/09/2020	09:37:51.490	-20.69	42.09	43.2	3.6	35.25	33.6	91.4	0.32	0.32
21/09/2020	09:56:54.010	-20.45	42.37	78.1	2.9	18.18	18.61	10.14	0.16	0.18
21/09/2020	14:22:25.390	-20.63	41.72	27.4	3.6	17.32	87.4	169.4	0.16	0.84
06/10/2020	19:11:51.390	-8.56	40.59	45.4	4.8	111.41	109.2	54.5	1.0	0.99
25/10/2020	15:45:27.860	-17.48	42.13	1.3	2.8	90.36	168.5	227.9	0.81	1.59
28/10/2020	01:28:33.150	-19.67	43.21	0.5	2.6	170.49	974.6	28.79	1.54	9.32
10/11/2020	02:40:13.310	-20.46	41.83	15.0	3.3	0.0	16.01	25.5	0.0	0.15
20/11/2020	13:06:25.510	-18.26	42.25	27.5	3.1	160.44	806.7	29.39	1.45	7.65
02/12/2020	01:36:53.370	-21.18	41.06	29.5	3.7	0.0	18.66	13.7	0.0	0.18
02/12/2020	01:36:54.070	-21.25	41.07	176.1	3.5	11.1	12.28	18.54	0.1	0.12
16/12/2020	04:50:59.890	-20.18	42.86	0.5	3.1	0.0	10.58	20.93	0.0	0.1

16/12/2020	04:51:00.970	-19.12	42.43	119.7	3.0	18.07	18.96	16.36	0.16	0.18
06/01/2021	03:17:32.270	-23.11	40.1	15.0	3.7	0.0	11.56	20.4	0.0	0.11
16/01/2021	10:09:15.290	-13.9	43.94	15.0	3.3	19.51	15.0	50.0	0.18	0.14
25/01/2021	04:01:51.130	-20.44	41.9	15.0	3.4	5.48	2.9	50.0	0.05	0.03
01/02/2021	23:52:05.610	-21.76	36.39	0.01	3.9	0.0	11.56	16.23	0.0	0.11
02/02/2021	01:06:14.340	-21.21	36.29	0.01	3.7	29.02	601.1	69.2	0.26	5.81
28/02/2021	08:31:04.660	-23.29	40.6	180.6	4.0	11.87	18.93	20.79	0.11	0.19
04/03/2021	06:20:07.000	-17.29	42.06	41.9	3.6	8.02	4.9	11.8	0.07	0.05
30/03/2021	08:45:55.500	-20.45	42.06	0.01	3.3	52.5	273.1	238.1	0.47	2.63
09/04/2021	16:46:14.440	-20.79	45.08	41.0	3.1	7.2	21.0	23.25	0.06	0.2
17/06/2021	16:26:16.840	-19.46	42.61	149.3	3.2	16.33	18.71	26.07	0.15	0.18
25/06/2021	22:29:14.380	-19.95	42.53	0.01	2.7	22.2	175.3	174.7	0.2	1.68
08/07/2021	04:21:32.500	-19.52	40.36	13.9	3.7	15.79	43.1	50.9	0.14	0.41
14/07/2021	22:29:48.100	-18.57	44.72	61.6	2.6	6.27	7.4	23.0	0.06	0.07
19/07/2021	09:23:58.860	-17.05	43.3	54.9	3.7	14.27	5.8	10.7	0.13	0.05
04/08/2021	12:10:12.430	-23.31	41.27	15.2	3.6	42.07	38.9	50.0	0.38	0.38
10/08/2021	23:56:48.960	-19.56	42.63	97.9	3.5	11.61	19.3	26.16	0.1	0.18
16/08/2021	16:24:23.490	-22.35	40.24	78.4	3.1	21.01	80.4	15.18	0.19	0.78
20/08/2021	10:41:41.900	-15.61	42.09	220.5	4.6	12.29	10.77	15.8	0.11	0.1
23/08/2021	10:29:36.490	-21.15	41.07	23.6	3.6	62.17	34.3	50.0	0.56	0.33
23/08/2021	14:17:59.270	-17.87	42.2	0.01	2.9	0.0	15.99	28.19	0.0	0.15
31/08/2021	18:52:55.290	-9.67	44.66	0.01	3.2	136.3	85.7	151.7	1.23	0.78
15/09/2021	01:30:36.800	-19.91	41.99	36.0	3.9	11.7	19.1	62.2	0.11	0.18
20/09/2021	04:36:46.070	-10.47	43.55	77.6	3.6	116.32	103.5	86.1	1.05	0.95
22/09/2021	08:30:54.400	-21.55	44.4	122.4	2.7	12.49	14.1	25.11	0.11	0.14
03/10/2021	06:57:01.450	-22.23	39.81	78.4	3.8	13.14	15.09	28.15	0.12	0.15
04/10/2021	09:19:39.120	-20.27	41.63	15.0	2.7	43.93	19.1	50.0	0.4	0.18
05/10/2021	21:38:03.840	-23.5	39.0	162.6	3.2	11.08	10.31	22.73	0.1	0.1
11/10/2021	12:33:22.900	-13.5	46.42	37.8	3.0	13.75	84.7	19.9	0.12	0.78

23/10/2021	01:31:01.760	-19.17	42.42	56.7	3.2	31.98	5.8	9.5	0.29	0.06
05/11/2021	06:37:32.220	-23.32	42.37	0.4	3.2	52.52	78.2	109.3	0.47	0.77
09/11/2021	13:12:23.410	-16.21	43.36	55.3	2.9	0.0	17.32	19.9	0.0	0.16
22/11/2021	00:47:59.910	-17.69	41.94	14.1	3.5	28.76	53.0	71.6	0.26	0.5
24/11/2021	05:43:08.510	-12.43	42.68	68.3	3.9	15.23	14.28	10.51	0.14	0.13
27/11/2021	23:08:09.280	-19.6	42.93	94.6	3.5	15.61	17.71	19.88	0.14	0.17

1